C-SIDE: THE CONTROL-STRUCTURE INTERACTION DEMONSTRATION EXPERIMENT

James B. Mohl and Hugh W. Davis
Ball Aerospace Systems Group
Boulder, CO

INTRODUCTION

The Control-Structure Interaction Demonstration Experiment (C-SIDE) is sponsored by the Electro-Optics and Cryogenics Division of Ball Aerospace Systems Group. Our objective is to demonstrate methods of solution to structure control problems utilizing currently available hardware in a system that is an extension of our corporate experience. The larger space structures with which Ball has been associated are the SEASAT radar antenna, Shuttle Imaging Radar (SIR) -A, -B and -C antennas and the Radarsat spacecraft. The motivation for the C-SIDE configuration is to show that integration of active figure control in the radar's system-level design can relieve antenna mechanical design constraints.

The radar system's effectiveness depends on the success of antenna orientation and structural motion control. Orientation control has been provided by the attitude control system of the supporting vehicle. Figure control has been passive by means of exotic materials, construction and deployment techniques. Active figure control, however, offers advantages from the standpoints of adaptability and enhanced response. For example, equipment-, crew- and maneuver-induced vibrations may be damped or anticipated to both steady the platform and maintain the figure of the radiating surface. Related applications where active structure control can be the final stage of a precision controller are large optical systems and pointing systems.

This presentation is primarily an introduction to the C-SIDE testbed. Its physical and functional layouts, and major components are described. The sensor is of special interest as it enables direct surface figure measurement from a remote location. The Remote Attitude Measurement System (RAMS) makes high-rate, unobtrusive measurements of many locations, several of which may be collocated easily with actuators. The control processor is a 386/25 executing a reduced order model-based algorithm with provision for residual mode filters to compensate for structure interaction. The actuators for the ground demonstration are non-contacting, linear force devices. Results presented illustrate some basic characteristics of control-structure interaction with this hardware.

The testbed will be used for evaluation of current technologies and for research in several areas. A brief indication of the evolution of the C-SIDE is given at the conclusion.

CURRENT SYNTHETIC APERATURE RADAR SYSTEM

The challenges when defining a spaceborne radar system are observing the packaging and launch weight constraints while maintaining precise geometry of the operational antenna. The current approach is to use very stiff antenna panels and to maintain strict alignment and thermal control. The fixed arrays are relatively heavy with sophisticated mechanisms for deployment from their launch envelopes. An example of the current technology is the Radarsat spacecraft shown in figure 1.

Radarsat is a Canadian Space Agency program to operate a synthetic aperature radar (SAR) satellite for research and commerical remote sensing applications. The C-band radar module, built by Spar Aerospace, has an antenna which is 15 meters tip to tip, 1.4 meters wide and supported from behind by an extendible support structure. The radiating surface is a series of waveguides which give it a steering capability in the elevation (cross-track) direction. Since the waveguides provide substantial structure, the operational antenna is quite stiff. The antenna's in-plane and out-of-plane bending modes occur near 4.2 and 5.2 Hz. The solar arrays are less substantial with out-of-plane and in-plane bending modes near 0.3 and 0.9 Hz. The attitude control system (ref. 1), in the bus module built by Ball Space Systems Division, has sufficiently low bandwidth to avoid interaction with the solar arrays and yet provides pointing stability to 0.1 deg. The primary attitude determination system provides attitude knowledge to better than 0.05 deg to facilitate registration of images by ground processing.

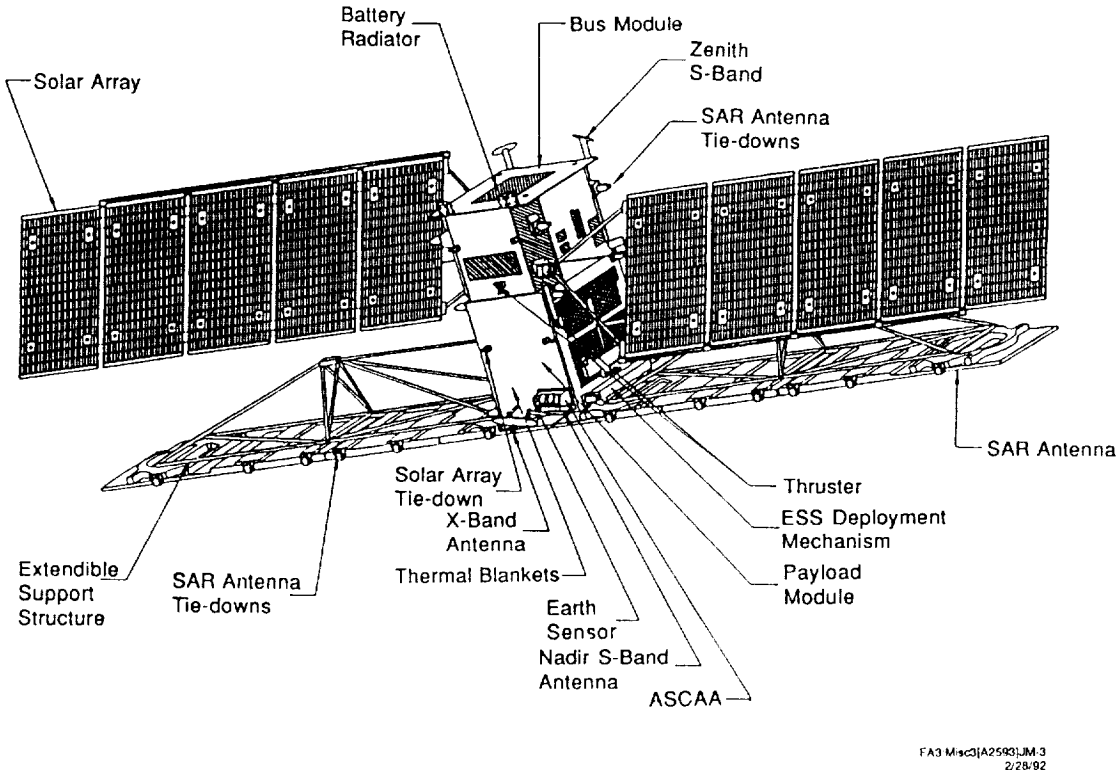

Figure 1. Radarsat uses precision deployment mechanisms and material stiffness to maintain antenna figure and strict attitude stability requirements for orientation control.

ACTIVE FIGURE CONTROL BENEFITS

A functional diagram for anSAR system is shown in figure 2. Microwave energy is generated, passed through the transmitters and phase shifters and radiated by the antenna to illuminate the target. The return energy is collected by the antenna, passed back through phase shifters and receiver and saved in mass storage. Some image processing is done on-board but much of the post-processing is a ground operation.

Benefits accrue from integration of active figure control through relief of antenna and spacecraft mechanical design constraints. A physically large antenna can have finer control to produce a more planar outgoing wavefront; shaping techniques to lower the sidelobes of the beam used in ground-based radars can be considered. Static misalignments at hingelines or distortion of panels can be readily removed; when extreme mechanical precision is not required, on-orbit assembly is an option. Low frequency, dynamic distortions can also be removed, such as those due to thermal shocks passing through an eclipse; this would reduce the need for strict thermal management. Lightweight construction or novel deployment options can be considered. Disturbance from the attitude control system, equipment or crew motion can be rejected so that operational restrictions can be relaxed.

The figure control system is independent of the radar function as shown by the loop at the bottom of figure 2. The sensors and actuators interface the antenna to the core structure. The figure control system maintains the position of the antenna relative to the core.

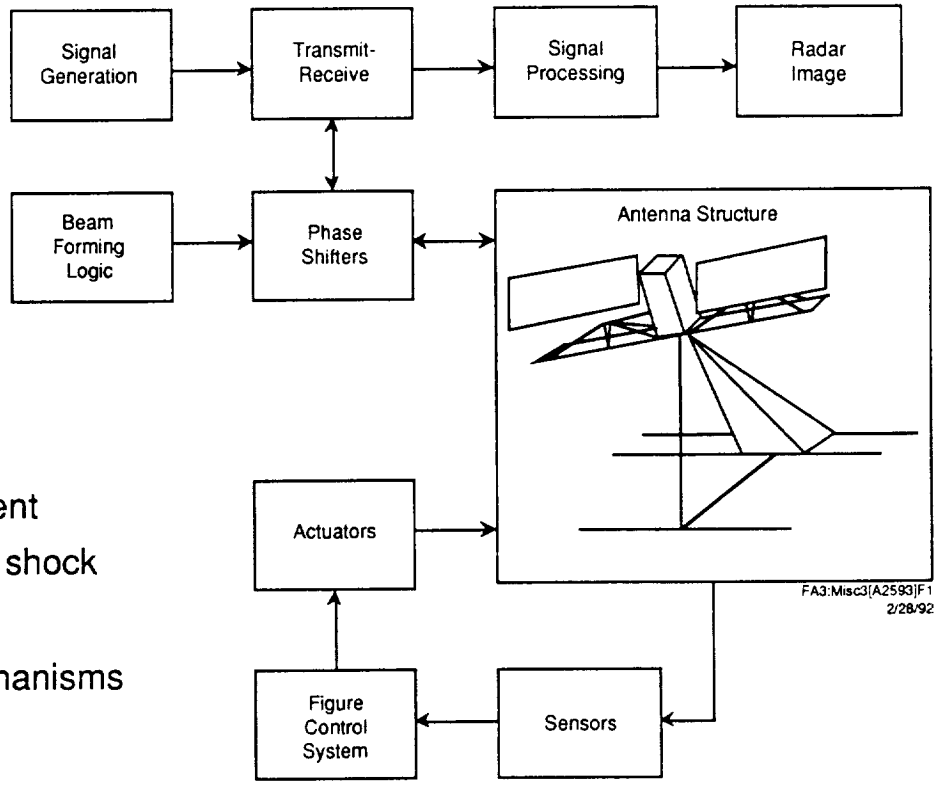

- Potential benefits
  - Larger antenna
  - Correct static alignment
  - Compensate thermal shock
  - Lighter construction
  - Lower precision mechanisms

Figure 2. Integration of figure control in the radar system definition relieves mechanical design constraints.

ENHANCEMENT FOR DISTRIBUTED ELEMENT RADAR SYSTEM

The radar platform contains the basic features of control-structure interaction that are the motivation for C-SIDE. However, there is an extension of the figure control capability peculiar to an antenna with a distributed element architecture. Control beyond the attempted correction of physical figure is possible because the radar system can use the results of the control process in a second path, shown in figure 3. The outgoing wavefront would become planar to fractions of a wavelength.

The figure control system uses a modal state estimator that can provide figure error estimates over the entire antenna face. The individual radiating elements receive phase shift commands appropriate for the estimated error at their physical position on the surface. Phase shifts of 1/32 of a wavelength are practical; that corresponds to a linear distance of 10 to 1 mm for an L- to X- band.

The spacecraft's attitude determination system provides the orientation of the core structure and defines the antenna boresight. This information could be used as other input to the beam forming logic to provide wide angle steering. Time delay in the transmission from widely separated portions of the array allows steering away from the antenna boresight. This has implication in the spacecraft design by allowing the antenna to be operated from a convenient attitude rather than being articulated by the vehicle.

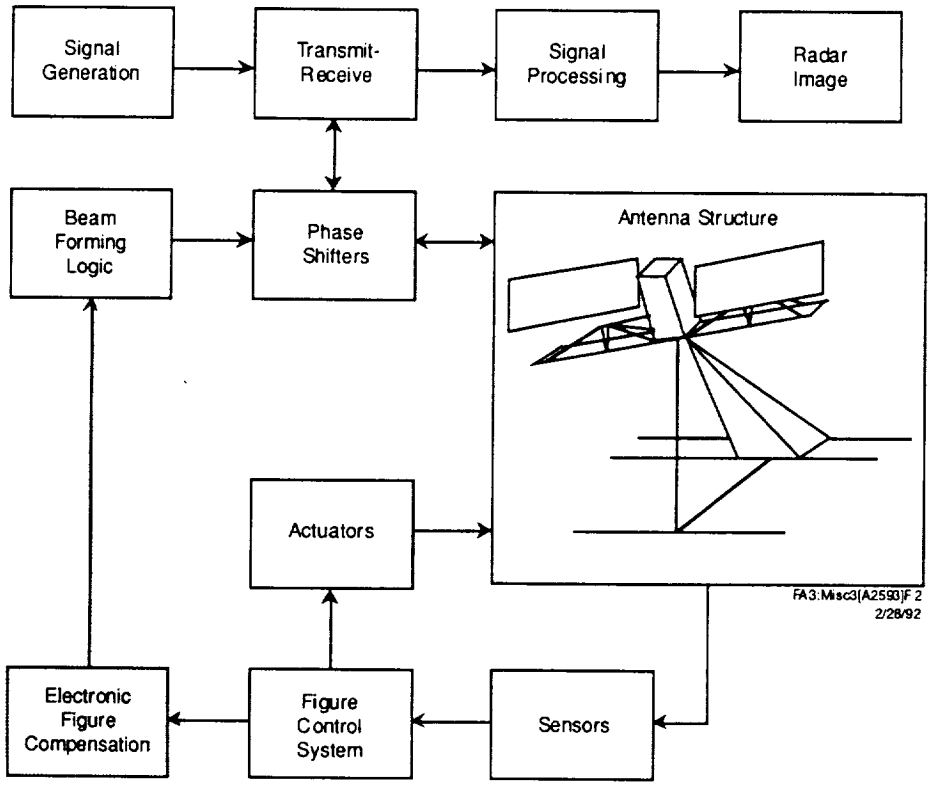

Figure 3. Figure control system facilitates on-board electronic compensation by the radar system for enhanced performance.

C-SIDE OVERVIEW

In the initial demonstration, we are assembling one-half of an antenna-like structure which is cantilevered from a massive central body as illustrated in figure 4. The "antenna" is a thin flexible facesheet one meter in height, three meters in length and 1.5 millimeters thick. A graphite/PEEK truss is placed behind the facesheet to act as a reaction structure. The figure control system is composed of a pair of single-axis Remote Attitude Measurement Systems (RAMS), up to ten linear force actuators and a single digital processor.

The physical size of our "large structure" is modest to reduce laboratory space requirements but is scaled to provide features modelling the large structure problem. The frequencies for the controlled surface start below 1 Hz. The low frequencies have the added advantages of reducing computational loading on the control system processor and lessening the impact of air damping in the laboratory environment. The reaction structure is specially fabricated to have bending frequencies starting in the neighborhood of the facesheet's sixth mode.

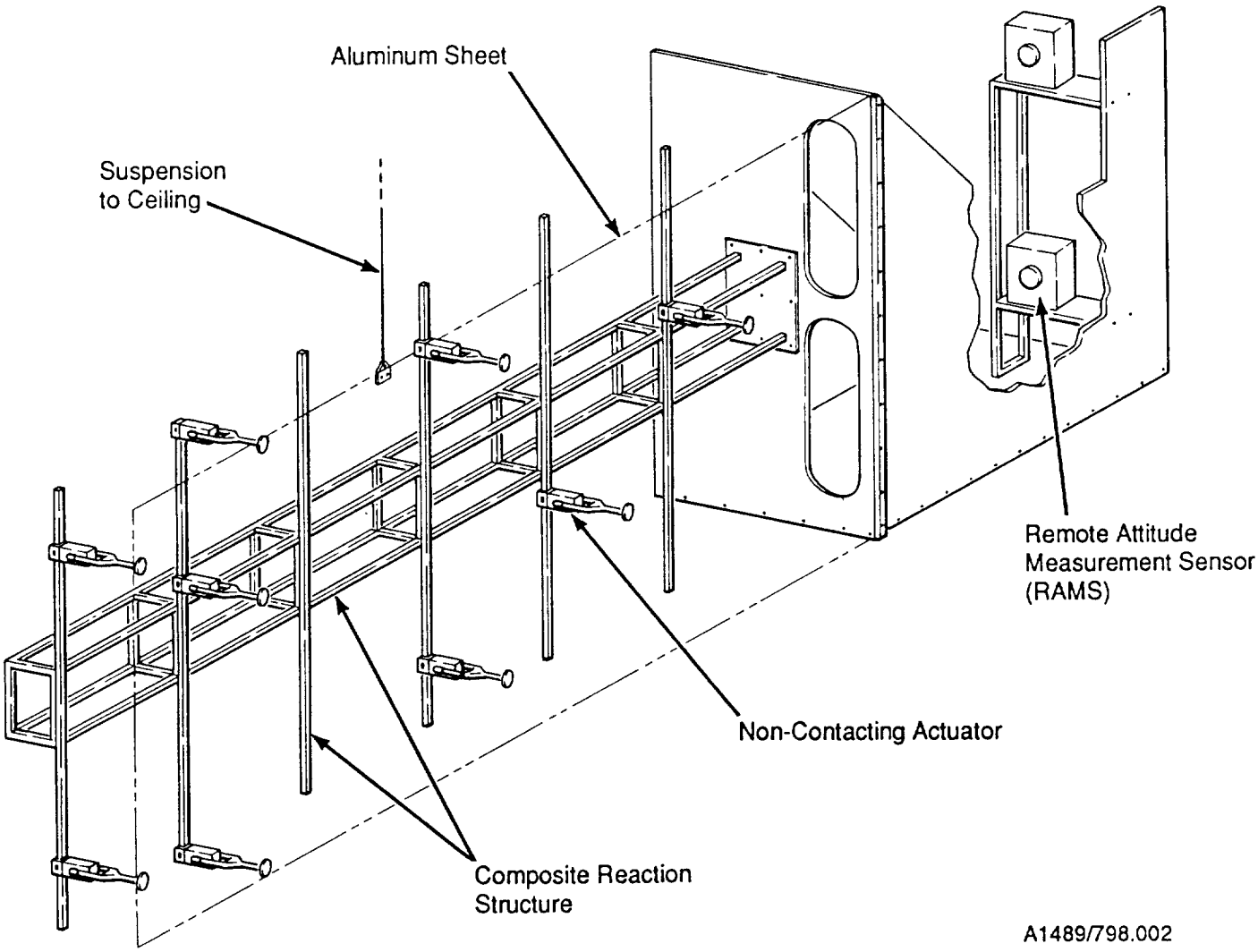

Figure 4. The C-SIDE is representative of a lightweighted spaceborne radar system that requires figure control of a thin, flexible plate supported by a structure from the rear.

FUNCTIONAL BLOCK DIAGRAM

The block diagram in figure 5 indicates the layout of the equipment and control system. The displacements of several facesheet locations are obtained by the RAMS by viewing targets on struts. The RAMS data is transferred through the interface box to the system controller. The controller interprets the RAMS data, performs the digital control algorithms and transmits the calculated actuator commands. The commands are distributed to the remote actuator drivers through the interface box. The actuators create motion in the facesheet and react on the reaction structure.

The interface box contains the force command decoder and the ±15 volt DC power supply. Its front panel allows access to the computer's analog input/output channels for use with the structural dyanmics analyzer. The ±24 volt DC actuator drive power is supplied externally.

The system controller is an 80386 with a coprocessor operating at 25 Mhz. There are three communication support cards. The digital I/O card is required for communication with the RAMS. One digital to analog channel is multiplexed for commanding the remotely located actuator electronics. Five other digital to analog channels are available for real-time display of selected "probe" points within the control algorithm. An analog to digital card allows injection of analog test signals and command waveforms into the digital system. MATLAB is available for control system design, data post-processing, analysis and documentation. Programming for the executable programs is done in Microsoft C 6.0.

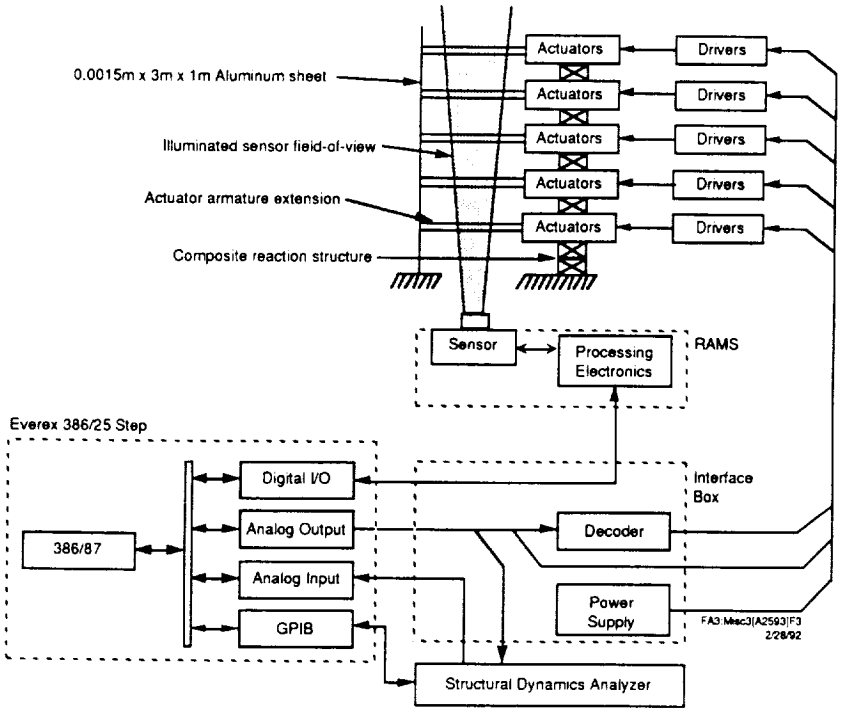

Figure 5. The initial C-SIDE provides physical figure control for the passive facesheet using a distributed array of actuators.

ASSEMBLED HARDWARE

Our control objective is to maintain the facesheet position, as measured by a remote sensor, by actuating against a well-behaved "reaction base" employing active or passive damping. Stiffness of the reaction structure provides one component of the reaction base with a passive "recentering" action. The mass of the reaction structure, augmented by the mass of cabling and drive electronics placed along its length, provides an inertial component to the reaction base. The reaction structure is placed well behind the facesheet to reduce interference with the RAMS field of view and to provide a standoff for actuator mounting. Abnormal stiffness is not to be required in the reaction structure as it is only necessary to maintain the actuators in the vicinity of their nominal positions.

Obtaining a stiff structure would not be a problem for this size of experiment. To get a better scaling for the large structure problem, a unique attribute of composite material fabrication is used to intentionally reduce material stiffness and lower the bending frequencies. The lamination orientation of the fiber is changed from alignment with the truss member axis to a 45 deg offset which reduces the modulus from 10 Mpsi to 2 Mpsi. The truss bay dimensions are small also, for appropriate scale: 0.11 m wide by 0.50 m long by 0.16 m high. The resulting modes shapes are: bending in the vertical plane at 2.8 Hz, first and second torsions about its long axis at 3.3 and 8.4 Hz, and bending in the horizontal plane at 4.0 Hz. The reaction structure is shown in figure 6. It is supporting its own mass of 11 kg and 65 kg of other components.

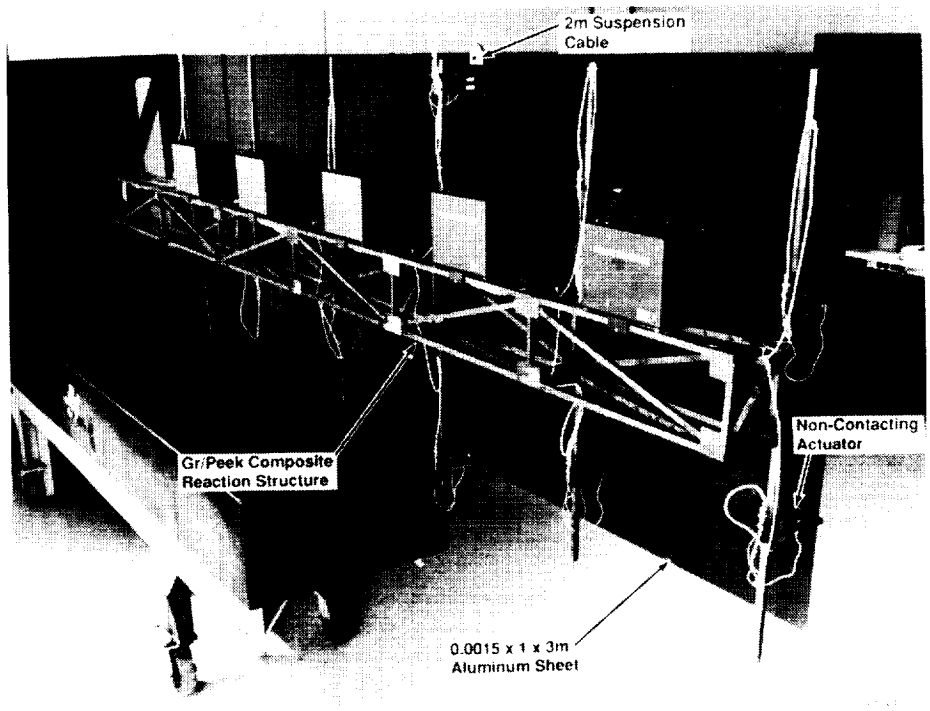

Figure 6. This view of C-SIDE shows the facesheet backside, reaction structure, actuators, drive electronics and cabling.

FACESHEET ACTUATOR

The non-contacting actuators shown in figure 7 reduce damping of the facesheet motion and avoid the nonlinear effects of stiction. The heavy, iron section (the stator) is attached to the reaction structure. The iron completes the magnetic circuit for two samarium cobalt magnets to establish a fixed field across the two air gaps. The light, coil section of the actuator (the armature) is attached to the facesheet by a yoke. The actuators produce force proportional to the coil current in the direction normal to the facesheet. The range of motion is ± 17 mm. The lateral and longitudinal clearances were modified in-house but are as small as practical to avoid compromising the actuator's force capability. Restraint of the facesheet motion is provided by the captured armature configuration. Overtravel snubbers protect the actuator element from excessive disturbance inputs (from overzealous observers). The force output capability is 2.5 N.

The armatures are mounted on spreader bars extended in the vertical direction from the reaction structure. The actuator locations are adjustable along the spreader bar. The connection of the armature to the facesheet is a slotted hole that allows small lateral adjustments.

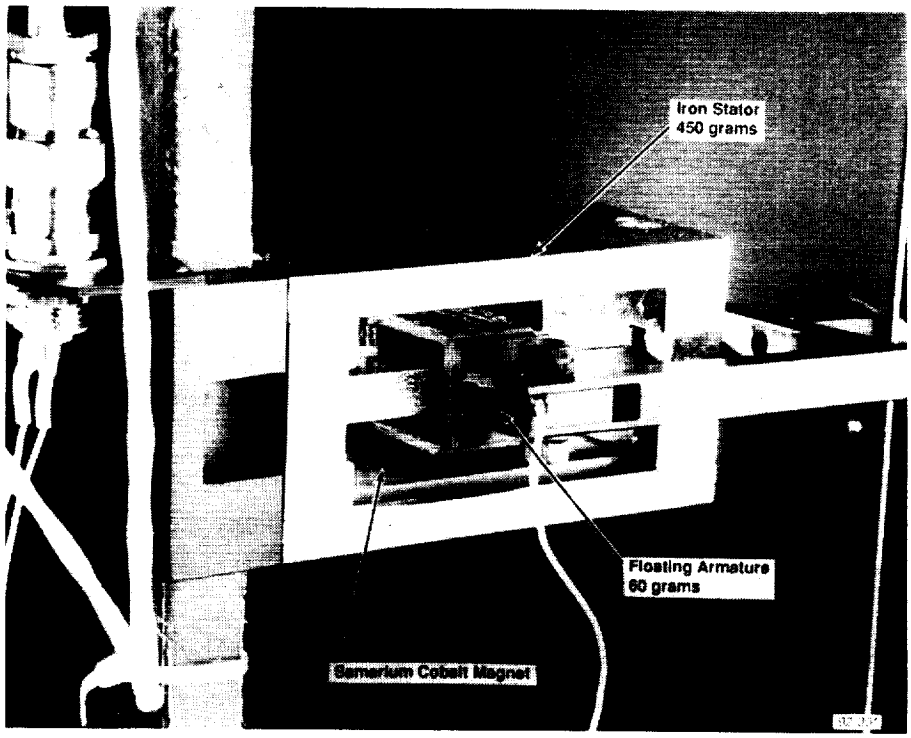

Figure 7. Non-contacting actuator reduces damping for demonstration purposes.

ACTUATOR DRIVE ELECTRONICS

Five remotely located decode and drivers electronics units are commanded from the control processor. Actuator commands are output in two parts. A single digital to analog converter channel transmits amplitude. A digital code is transmitted simultaneously to select the actuator drive circuit which reacts to the command. The five remote driver boxes each support two actuators. Each box contains sample and hold circuitry, to maintain the force command amplitude between updates, and linear drive, current loop electronics to energize the actuators. Figure 8 shows the closed loop bandwidth of the current loop is 32 kHz; actuator gain and phase errors can be ignored since our frequency range of interest will be below 100 Hz.

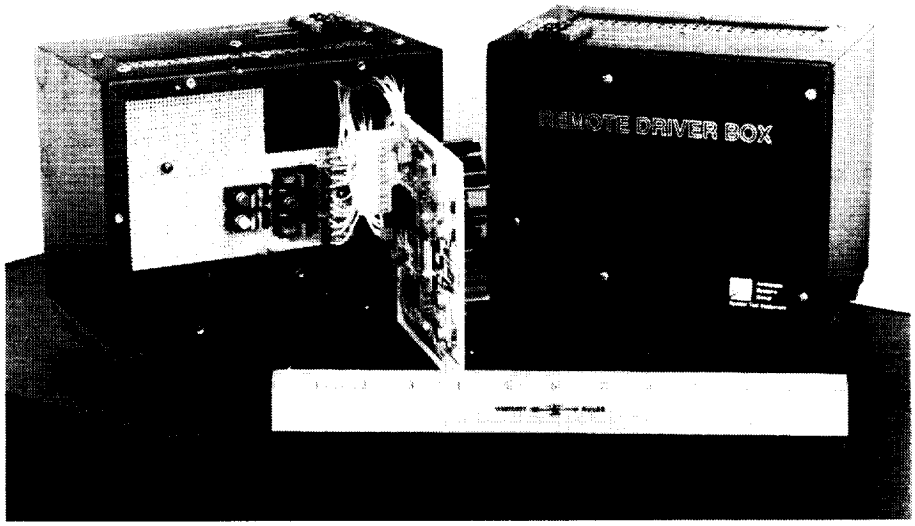

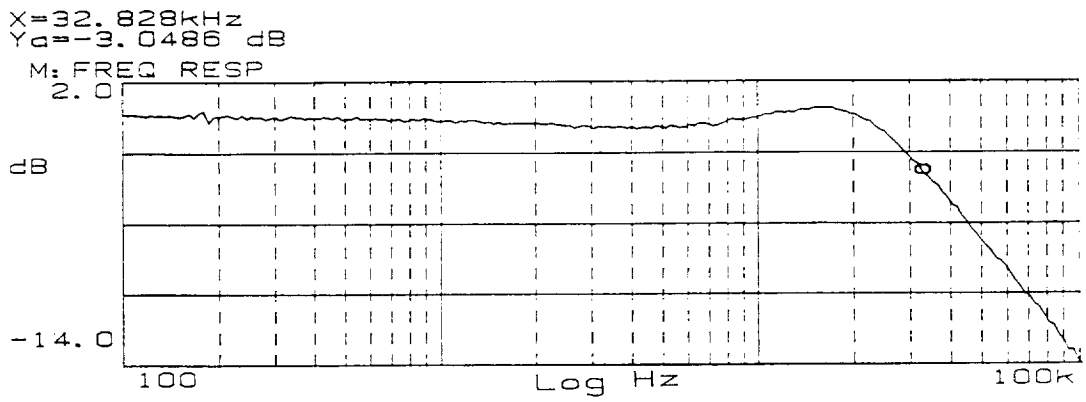

Figure 8. Actuator drive reponse is unity gain for frequencies below 10 kHz. No adjustment for actuator dynamics is required in system modelling.

REMOTE ATTITUDE MEASUREMENT SYSTEM

Measurement of the facesheet surface figure is required for feedback to the control system. RAMS can provide data for a small number of target locations at a high rate (to capture local, high frequency motions) or data for many targets at a lower rate (for identification of distributed effects over the entire structure). The passive retro-reflective target tape used by RAMS is lightweight and can be located on the actuator armature. It eliminates the added complexity and weight of power and signal lines to each sensor location.

The RAMS optics are positioned to view most of the facesheet backside and a portion of the reaction structure. A single-axis RAMS is sufficient for this case since only facesheet-normal translations are of interest; the location of targets in the other two dimensions on the facesheet can be measured. An operational schematic for RAMS is shown in figure 9. The view shown would be looking down from the ceiling for the C-SIDE installation. The RAMS boresight is at a high angle of incidence so that the field of view fans out over a large target area. The resolution in the sensitive direction varies along the facesheet. The worst condition is at the free end, farthest from RAMS; motions of 0.015 mm are resolvable there. Targets on the facesheet are placed on the actuator armature yokes. Targets on the reaction structure are also provided for system identification. The view looking out of the RAMS porthole is shown at the right of the figure.

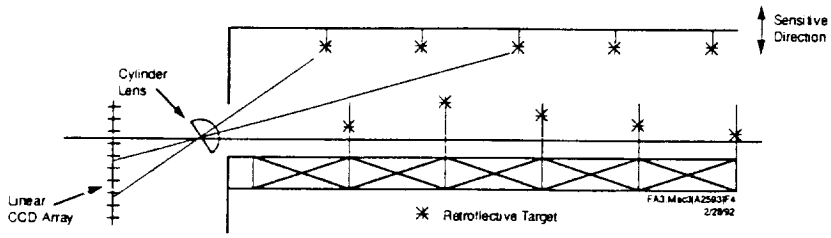

Exaggerated Top View

- Insensitive to vertical target placement
- Resolution is most coarse for distant targets

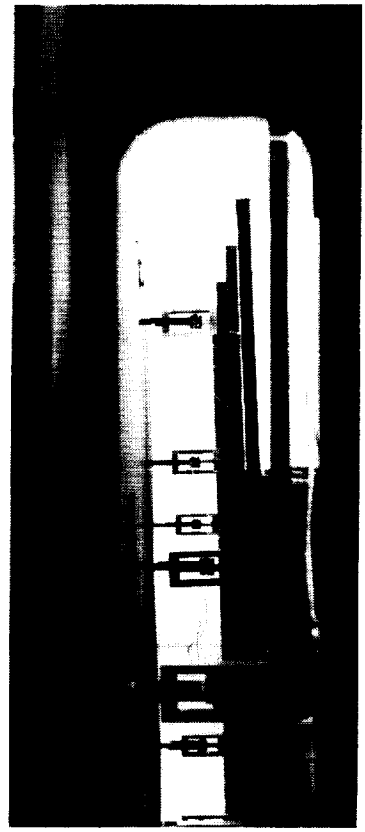

Figure 9. Each single-axis RAMS measures horizontal position at actuators and locations on the reaction structure.

The orientation of the facesheet is chosen to reduce modification to the familiar low frequency "cantilevered modes". However, this requires the facesheet to be supported along its length to prevent buckling due to gravity. Lateral stiffness of the support is reduced by using a long suspension wire with only small displacements being allowed.

The facesheet is solid aluminum stock, rather than honeycomb, expressly to create low frequency modes. The mass of the facesheet is less than 14 kg and needs only a single support wire at 2 m from the base. The support wire length is limited by the lab ceiling height to about 2 m. NASTRAN results for this thin, constrained, cantilevered beam under the influence of gravity are given as mode shapes in figure 10. The first and second modes are predominantly cantilevered beam modes occurring at 0.28 and 0.89 Hz. The third mode is torsion about the longitudinal axis at 1.08 Hz. The fourth mode is another beam mode at 2.55 Hz. The fifth and sixth modes are torsional.

Note that compensation for gravity has a major qualitative effect on the experiment. If the facesheet were in zero-g, NASTRAN would predict the first beam mode at 0.15 Hz and the first torsional mode at 0.8 Hz. The support wire adds significant resistance against the first beam (effectively quadrupling the stiffness) and causes a neutrally stable torsional mode to become a stable double-pendulum-like mode.

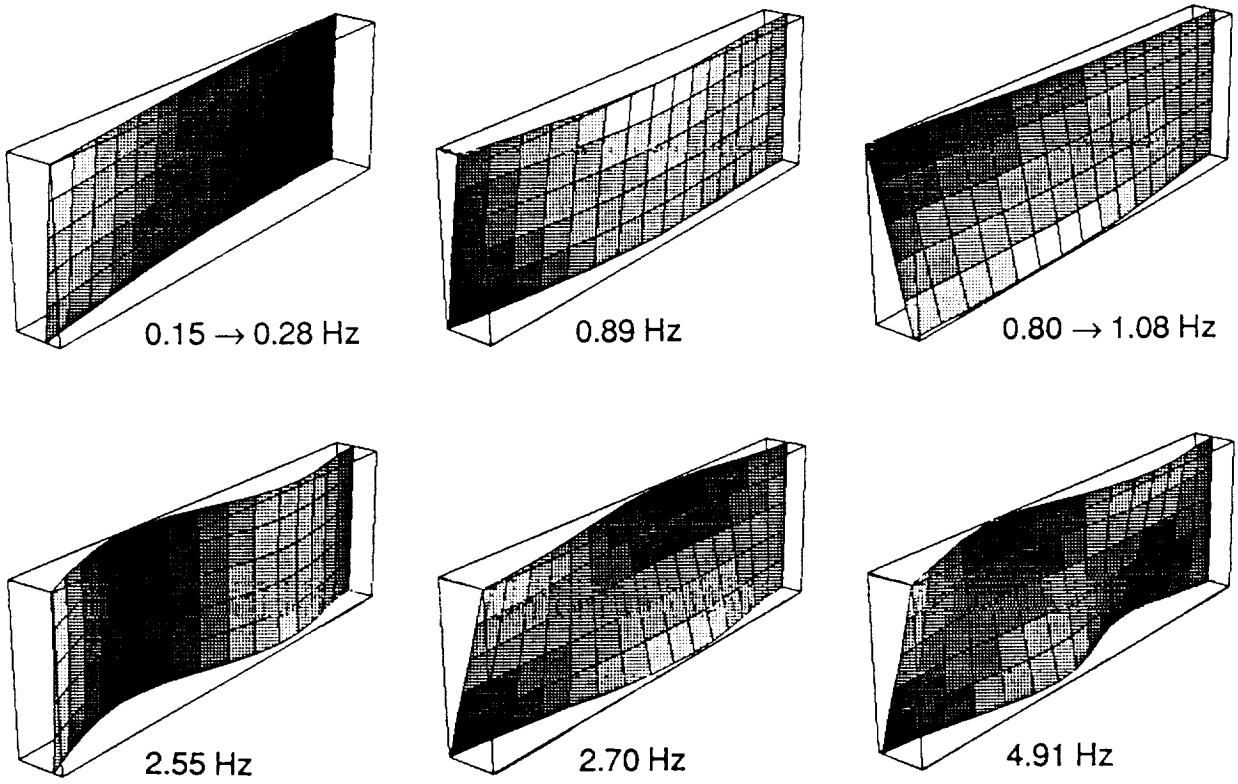

Figure 10. Suspension cable modifies the first cantilever and torsional mode frequencies most significantly.

REDUCED ORDER MODEL-BASED CONTROL

The control algorithm is based on a reduced order model of the significant vibration dynamics of the facesheet represented in modal coordinates. The definition of "significant" is determined by the system performance requirements. For the purposes of demonstration, the control actions are applied so that disruptive interaction with unmodelled flexible dynamics occurs. It is subsequently suppressed to restore desirable performance.

The context of the ROM controller is given in figure 11. The system to be controlled includes the actuator and sensor dynamics as well as those of the structure. The ROM controller takes a subset of the system dynamics, which must include any open-loop unstable modes, to be used in an state estimator model. It receives a set of measurements from the system and returns a set of actuation commands. A by-product of the process is its estimate of physical measurements at the sensors (and possibly other locations) for the modelled modes. The states of the estimator can be given an external reference command to position the system. This general configuration can be viewed as the control system for the figure of a surface, the pointing of a gimbal set, or the rigid body attitude of a spacecraft.

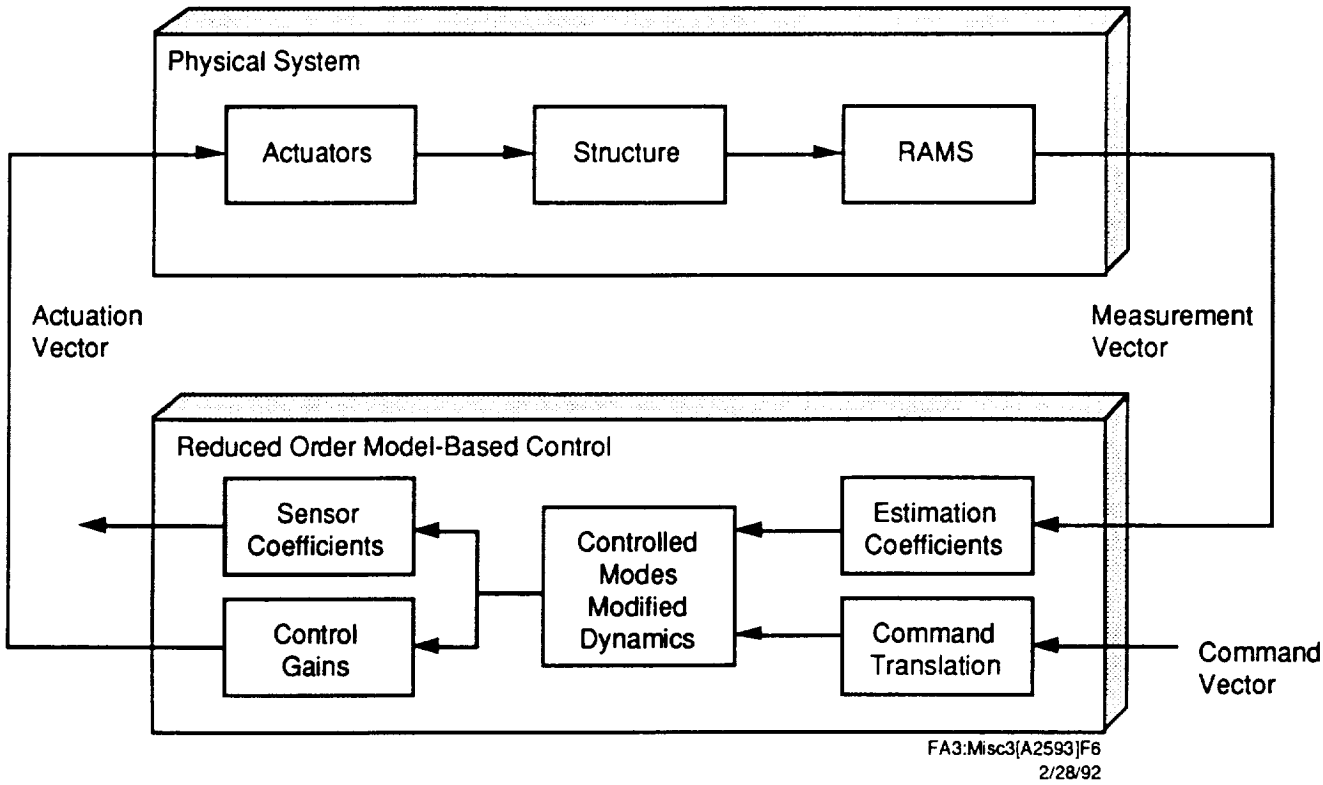

Figure 11. Reduced order model-based (ROM) control processes sensor measurements to define actuation commands.

CONTROL FOR FIRST TWO MODES

The performance objective for the initial demonstration is to increase the response frequency and damping of the first two beam modes of the facesheet. MATLAB's pole placement routine defines gains for the ROM controller. The algorithm selects the actuator and sensor locations with the highest modal gains. To control the first two modes, two collocated actuator-sensor pairs are used: at the free end of the facesheet and at the bottom below the suspension cable.

Pole placement is so aggressive in this case that it gives a pathologically interesting result. The root locus for the combined controller and structure model is shown in figure 12 with the control gains being varied from 0 to 100 percent of their design values. The first seven modes of the facesheet are used with a natural damping of 1 percent assumed. The first and second modes begin migrating in the desired direction. The third mode is immediately driven unstable. The interaction with unmodelled dynamics at higher gains causes the controlled modes to move to the right and destablizes the first mode. Some damping is applied to higher frequency cantilever modes while higher frequency torsional modes are slightly destabilized.

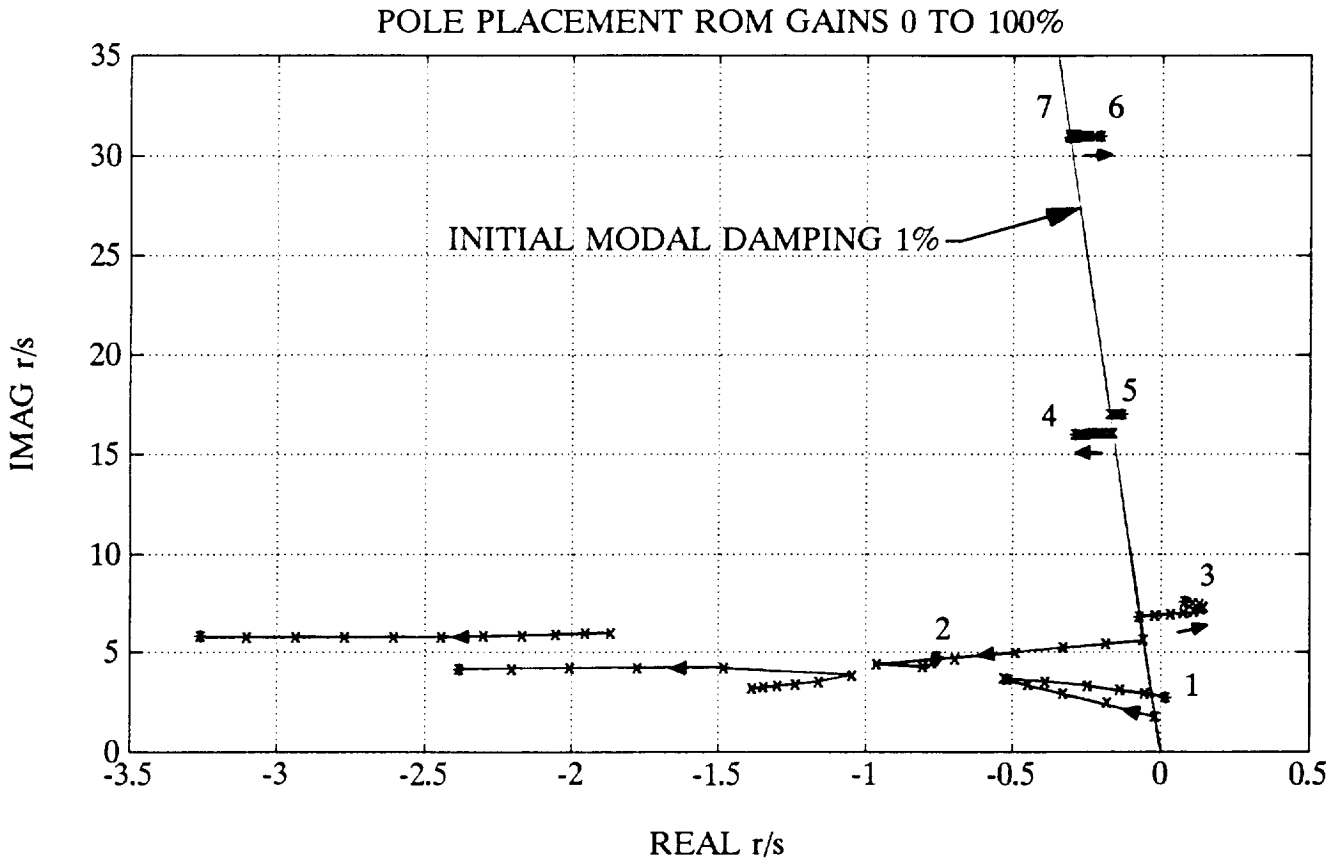

Figure 12. ROM control is intended to add damping and stiffness to the first two modes. Interaction with dynamics not modelled in the controller causes instability in both the first and third mode.

ROM CONTROL ALONE

The response for this ROM controller alone is unstable as expected. The result in figure 13 is the response to a 1 N, 0.02 sec pulse applied at the free end of the facesheet, 30 cm below center. This location drives all the cantilever and torsional modes well. This same perturbation is used for the other transient cases to follow. The sensed position and input locations are shown below.

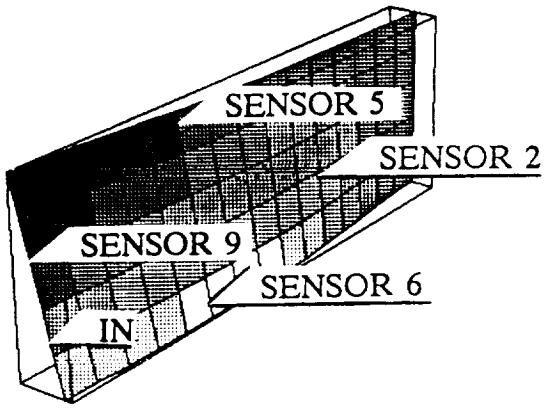

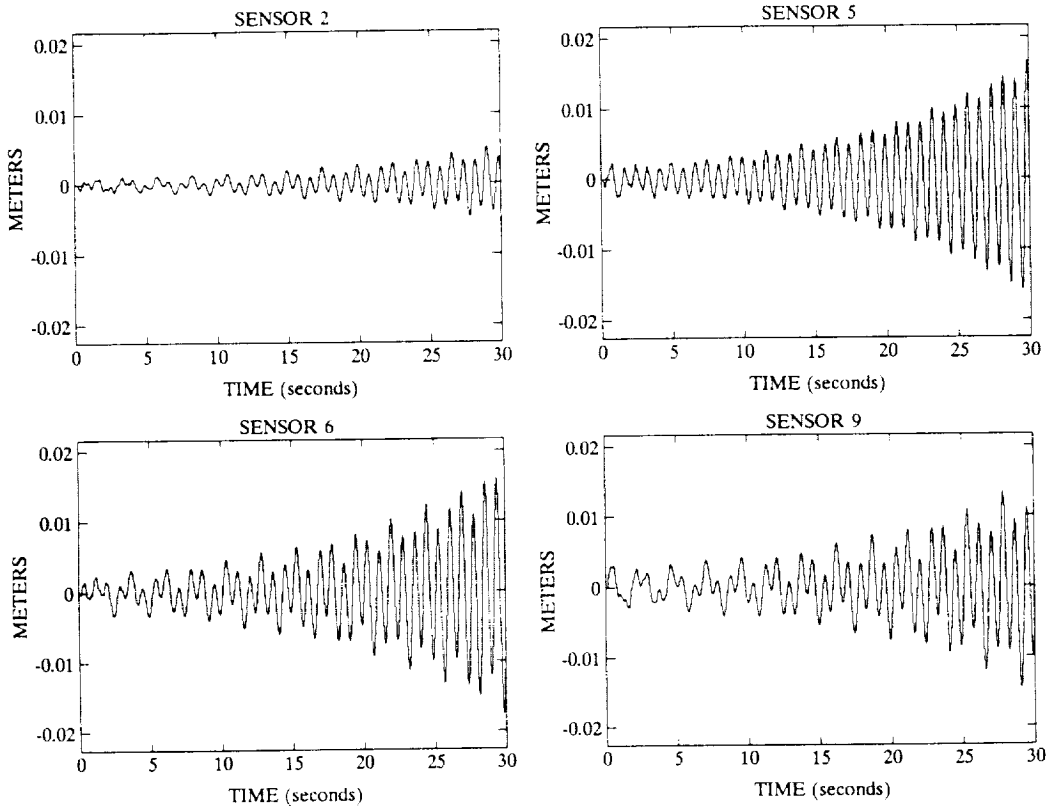

Figure 13. The pole placement design ROM controller alone cannot recover from a perturbation.

RESIDUAL MODE FILTER

The ROM design ignores the effect the control system may have on the rest of the modes of the structure, i.e., the residual system. As was shown, it is possible for some small number of the residual modes to be driven unstable by the ROM controller. The residual mode filter (RMF) is introduced at this point to correct the problem (ref. 3). The RMF is added in parallel to the controlled system, as shown in figure 14, to process the commanded control action and define expected responses at the sensor locations. The signal is subtracted from the incoming sensor measurements, having the effect of opening the feedback path for the destabilized modes. This action returns the destabilized modes to their uncontrolled, stable response character. The RMF signal is well-phased to actual motions and does not suffer from the phase error introduced by a series notch-filter.

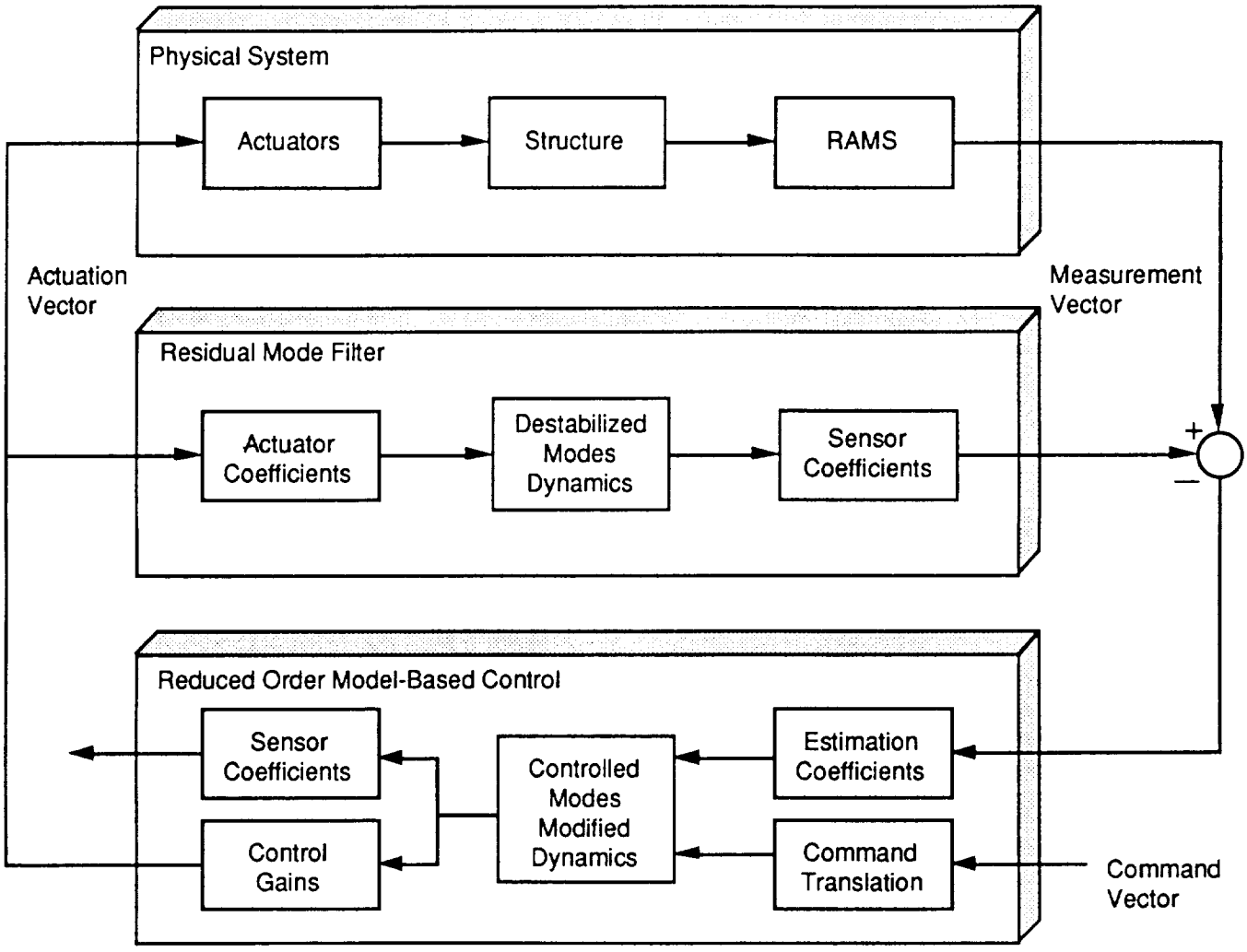

Figure 14. Residual mode filter (RMF) removes destabilizing interaction with unmodelled dynamics.

The root locus for inclusion of the RMF in figure 15 shows the third mode returns to its uncontrolled location. Removal of the strong third mode interaction allows the controlled structural modes and the state estimator poles to migrate toward their intended positions. In general, these roots approach, but do not achieve, the locations specified in the ROM control design. This is due to the remaining interaction with stable, uncompensated, high frequency modes. This is not usually a notable discrepancy because the interaction is seldom so severe.

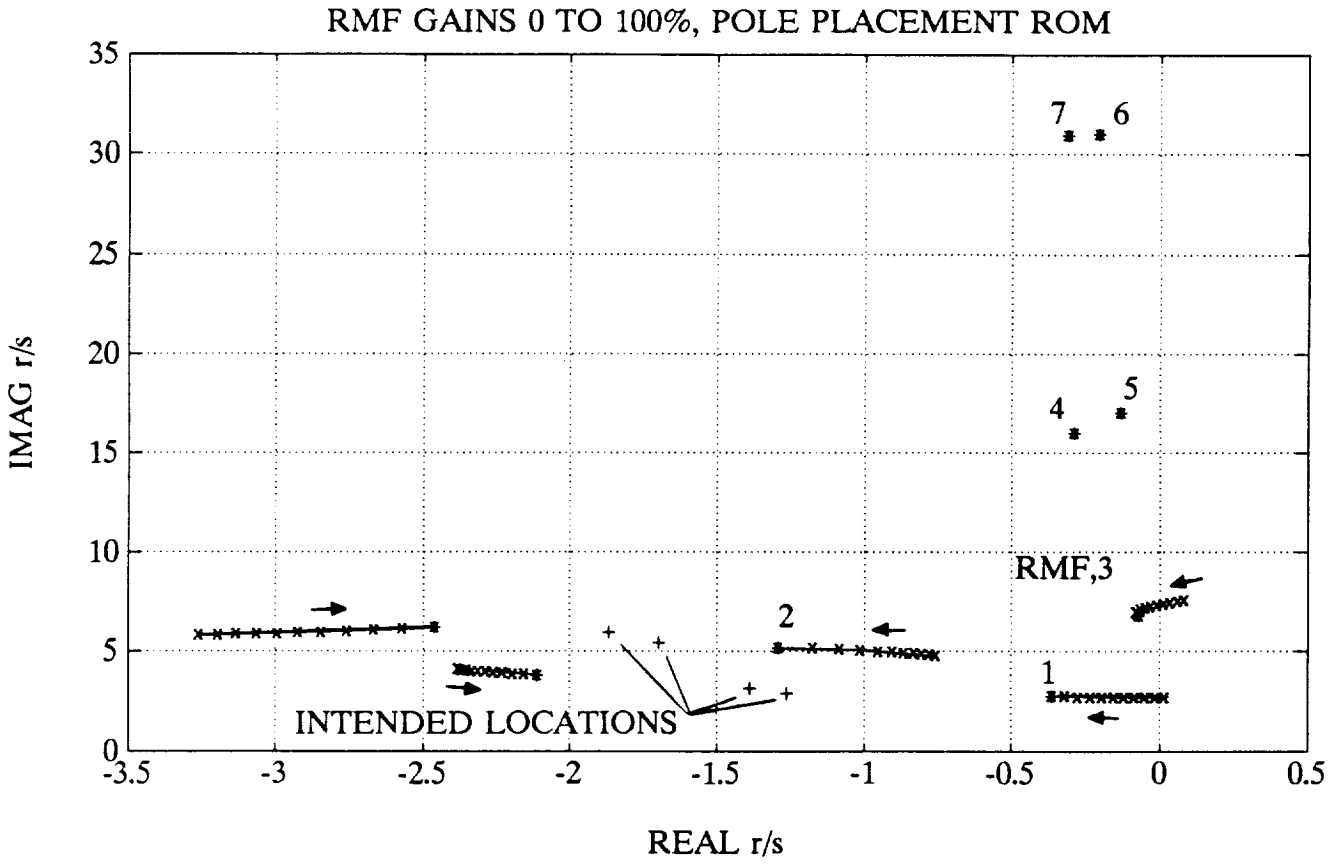

Figure 15. The RMF returns the third mode to its uncontrolled character and allows the first mode to become stable.

RMF REMOVES INSTABILITY

The response given in figure 16 is for the same perturbation as before. It is stable now but the performance is hardly acceptable. This result motivates a second design that includes control of the third mode.

This example is included as a reminder that residual modes can be driven by the ROM control. For the present case, the second mode control frequency is essentially the same as the uncontrolled third mode. Energy used for damping the second mode is also input to the third mode. The amplitude of the third mode excursion continues to increase until the control input for the second mode settles. Residual mode motion persists until it can be damped by material properties.

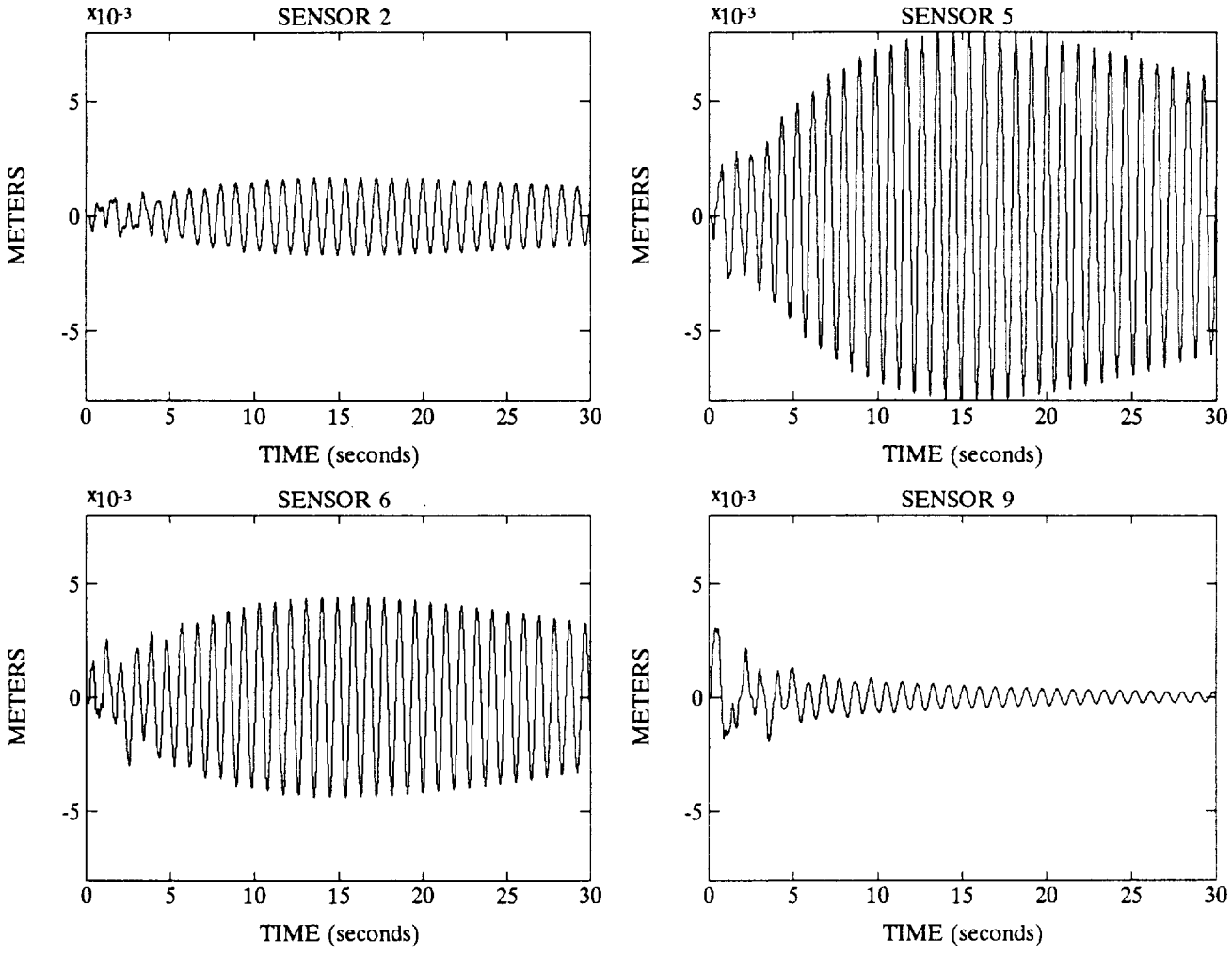

Figure 16. Control for an impact at the free end of the facesheet drives the uncontrolled residual mode. This motion will be damped by mechanical properties only.

LQR CONTROLLER

A pole placement design for three modes could be used and is better behaved than the preceding case. However, consider a frequency weighted (ref. 4) linear quadratic regulator (LQR) and estimator design for the first three modes. The weightings, in the Q matrix of the performance index for the modal displacement and velocity states, are set as the square of each mode frequency. The control weightings, in the R matrix, are the identity matrix multiplied by a parameter, α. The LQR solution is less aggressive and drives controlled roots to the left on the root locus plot along trajectories of constant frequency; the damping factors for all controlled modes increase at approximately the same rate. An RMF is not required for this design with $\alpha = 1$.

The response for the same pulse is shown in figure 17. This ROM controller settles quickly to the desired flat surface figure. The fourth and fifth modes are harder to drive with commanded actuation so there is little residual motion.

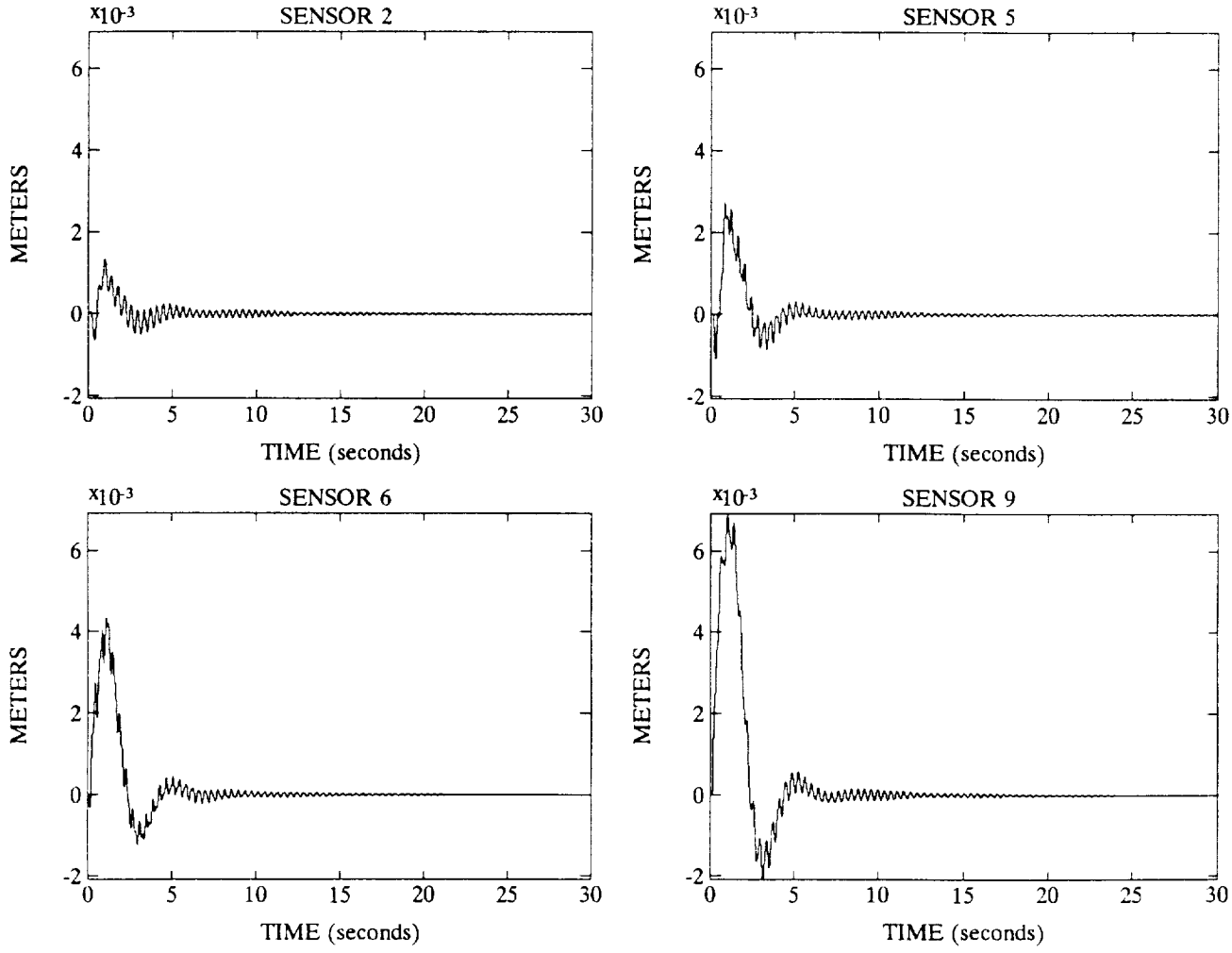

Figure 17. The LQR controller designed to create equal damping coefficients for the first three modes succesfully recovers from the impact.

FUTURE DIRECTIONS

The immediate usage of C-SIDE is for technology evaluation and research in several areas: structures, actuators, sensors, control, and processing.

The composite structure was fabricated under a separate internal development effort. It may be upgraded as new materials and fabrication methods are investigated and converted to an active (smart) structure. Current activities include embedded, distributed actuation and sensing. Eventually, these may be incorporated in an active facesheet.

Possibilities for future enhancements to the sensing capabilities include alignment transfer, inertial sensors and local sensing at the actuators. There is interest in using combinations of RAMS units to provide alignment transfer from a remote "navigation base" back to the core structure. Inertial sensors may be used to stabilize the structure against local laboratory vibrations. This is of interest for isolated benches in optical experiments. Local position sensing can be added at the actuators. The relative position is useful in localized control to recenter the actuator at low bandwidth or in a distributed control to drive an active reaction structure.

Several different actuator mechanisms can be applied to the structure and interfaced to the control system. A precision actuator for the reaction structure is a small reaction wheel. Interesting issues here are the effect of stored momentum during repositioning of structure sections and momentum unloading schemes. Active struts may be used as a primary control source between the facesheet and reaction structure or at the root of the structure. Thrusters probably are most applicable for coarse positioning of the reaction structure behind the vernier positioning system on the facesheet. Experience with many actuators types will enable recognition of novel solutions to difficulties in current and future products.

C-SIDE will provide experience with various strategies for ROM design such as variations on the basic LQR, Positivity and H_∞ methods. We are also investigating system identification techniques such as the eigensystem realization (ref. 5) and residue identification (ref. 6) algorithms. We have had success with feedforward and recursive neural networks functioning as RMFs in the C-SIDE simulation (ref. 7); verification with the hardware is planned for this year. Research areas include adaptive residual mode filters and the possibility of control during assembly of an additional structure.

Computational capabilities can be increased by segregating the control functions. The formulation of the ROM structure model and RMF bank lends itself to use of parallel processors. Additional control functions, such as disturbance accommodation and system identification, can be delegated to other processors with results being passed to the main control processor.

Although control-structure interaction is most often associated with large, flexible space structures, it is not necessary to narrowly limit its consideration. The expertise developed on C-SIDE is transferable to other high performance products: whenever a structure supports, or is itself, an actively positioned device. With processing speed increases, parallel processing and hybrid circuitry, the control method will be targeted at smaller structures also.

REFERENCES

1. Mohl, J.B.; Dieter, R.J.; and Muckle, A.M.: Attitude Determination and Control for the Radarsat Spacecraft. AAS 92-011, Feb. 1992.

2. Davis, H.W.; Sharkey, J.P.; and Carrington, C.K.: Structural Control Sensors for CASES. AAS 90-044, Feb 1990.

3. Balas, M.J.: Finite-Dimensional Controllers for Linear Distributed Parameter Systems: Exponential Stability Using Residual Mode Filters. *J. Math. Analysis and Appl.*, 1988.

4. Mackison, D.L.: Guaranteed Cost Control of Flexible Space Structures. PhD Thesis, University of Colorado - Boulder, 1988.

5. Juang, J.-N.; and Pappa, R.S.: An Eigensystem Realization Algorithm for Modal Parameter Identification and Model Reduction. *J. Guidance, Navigation and Control*, Vol. 8, No. 5, Sep.-Oct. 1985, pp. 620-627.

6. Medina, E.A.; Irwin, R.D.; Mitchell, J.R.; and Buckley, A.P.: MIMO System Indentification Using Frequency Response Data. AAS 92-065, Feb. 1992.

7. Bowman, C.; and Roorda, J.J.: Spacecraft Smart Structure Neural Network Adaptive Control. *Proc. of Government Neural Network Symposium*, Huntsville, AL, Sep. 1991.